studies (Moskalenko et al. 2001)—the posterior PDF of L extends from 25 to 85 kpc for model III (most probable value at 46 kpc). In terms of statistics, the best-fit model is stil model III, for which the χ^2/d.o.f is 1.41.

Modified DM ($r_h \neq 0$): the presence of a local bubble results in an exponential attenuation of the local radioactive flux, see Sect. 2.3 and Eq. (10). We thus expect to have a different best-fit parameter for L in that case. The resulting posterior PDFs of L and r_h and the correlations to the propagation parameters for this modified DM are given in Figs. 6 and 7 for models II and III respectively. The most probable values are gathered in Table 7 (third and last lines).

As expected, the local bubble radius r_h is negatively correlated with the Galactic halo size L. The effect is more striking for model III, where the favoured range for L extends from 1 to 50 kpc. The most probable value is 8^{+8}_{-7} kpc for a local bubble radius $r_h = 120^{+20}_{-20}$ pc. The χ^2/d.o.f of this configuration is 1.28, instead of 1.41 for the standard DM. The improvement to the fit is statistically significant according to the Fisher criterion.

The situation for model II is different. The halo size L is already small for the standard configuration $r_h = 0$. Adding the local bubble radius r_h to the fit decreases the most probable value of L only slightly to 4^{+1}_{-1} kpc and the measured value of r_h is compatible with 0 pc. In addition, the χ^2/d.o.f is 3.69 and hence poorer than for the configuration without the local bubble feature. In this model (diffusion/reacceleration, no convection), a local underdensity is not supported.

5.1.2. Results and comparison with fits to ^{26}Al/^{27}Al and ^{36}Cl/Cl

We repeat the analysis for the remaining isotopic ratios. The resulting marginalised posterior PDFs of the Galactic halo size L and the local underdensity r_h are given in Figs. 8 and 9 for models II and III, respectively. The correlation plots with the transport parameters are similar to those of Figs. 6 and 7 and are not repeated.

Standard DM ($r_h = 0$): as for the ^{10}Be/^{9}Be ratio (red-dotted line), L is well constrained in model II at small values for the ^{26}Al/^{27}Al (green-long dashed-dotted line), and ^{36}Cl/Cl (blue dashed-dotted line) ratios, covering slightly different but consistent ranges from 4 to 14 kpc. The width of the estimated PDFs increases when moving from the ^{10}Be/^{9}Be ratio to the ^{36}Cl/Cl ratio, due to the decreasing accuracy of the data. In the same way, the adjustment to the data becomes poorer, as expressed by the increase in χ^2/d.o.f from 3.59 to 4.09. Used alone, the radioactive ratio ^{10}Be/^{9}Be constrains the most precisely the halo size L, but the constraints obtained with the other radioactive ratios are completely compatible within the 2σ range. The most likely value of L is ascertained when the three radioactive ratios are fitted simultaneously (black solid line).

The best-fit model is model III, where the overall covered halo size range extends from 20 to 140 kpc. The most probable value found for L with 68% confidence level (CL) errors is 62^{+7}_{-10} kpc.

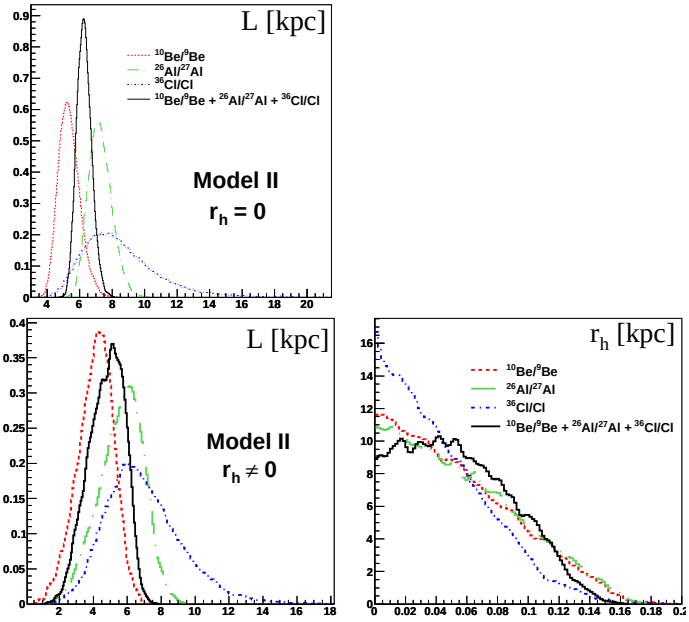

Fig. 8. Model II: marginalised posterior PDFs of the Galactic geometry parameters for the standard DM ($r_h = 0$, top panel) and for the modified DM ($r_h \neq 0$, bottom panels). The four curves result from the combined analysis of B/C plus isotopic ratios of radioactive species: B/C+^{10}Be/^{9}Be (red dotted line), B/C+^{26}Al/^{27}Al (green long dashed-dotted line), and B/C+^{36}Cl/Cl (blue dashed-dotted line). The black solid curve represents the extracted PDF resulting from a simultaneous fit of B/C plus all three isotopic ratios. All PDFs are smoothed.

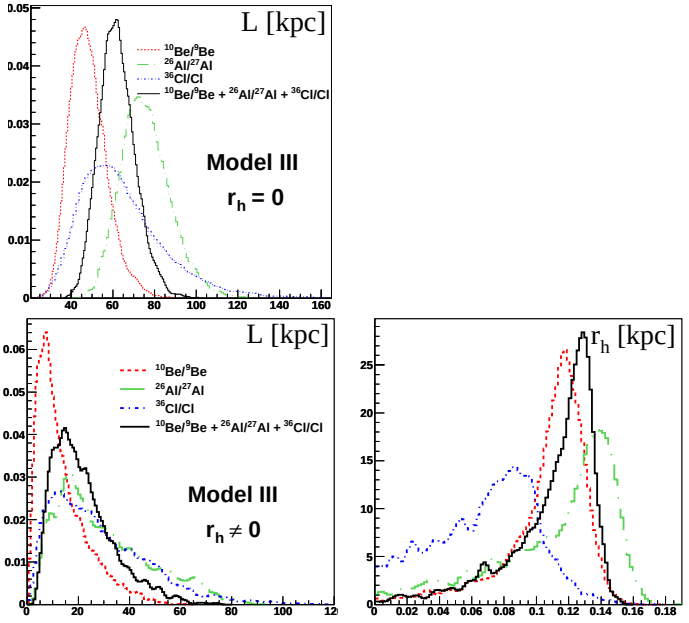

Fig. 9. Same as in Fig. 8, but for model III.

Modified DM ($r_h \neq 0$): the resulting marginalised posterior PDFs of L are shown in Figs. 8 and 9 (lower left) for models II and III, respectively. Again, the extracted PDFs for all radioactive ratios are completely compatible for both models. As described above, the decrease in L is more pronounced for model III than for model II. This decrease can